consistent with the correlation time for the dipolar term being dominated by the rotational correlation time for the complex ion since values for the rotational correlation time are expected to be in the several tens of picoseconds range.[35,36]

The data of Figure 2 are shown again in Figure 3 normalized to the number of water molecules bound to the metal at each pH value. It is now clear that the data fall into only two classes, those below pH 10 and those pH 10 and above. The relaxation dispersion data for samples with pH between 3 and 9 are coincident with pH 3. These data show that the relaxation efficiency of the metal center remains essentially unchanged as the monomeric complex is formed. This observation is consistent with the effective correlation time for the electron–nuclear coupling being that for rotation. However, the relaxation efficiency increases significantly when additional water is displaced by the association reaction even though the metal centers are brought close together in the dimer.

It is likely that the high pH product is predominantly a dimer of the μ-hydroxo or μ-oxo type previously reported for EDTA complexes.[37] The properties of transition-metal dimers and their magnetic relaxation properties in particular have been discussed by several groups.[38-40] One might assume that the relaxation rate in the dimer should double because each proton in the bridging position may interact with two electron magnetic moments instead of one. The concern in such a dimer for transition elements is that the electrons will antiferromagnetically couple, making the effective electron magnetic moment much smaller, the consequence of which would be a decrease in the efficiency of the metal-center-induced relaxation. However, in the present case, the relaxation efficiency is higher in the dimer, which is consistent with the general unimportance of antiferromagnetic coupling for the lanthanide complexes.

Inspection of Table I shows that neglecting special effects of the dimerization reaction leads to an intermoment distance of 2.6 Å, which is considerably shorter than expected for lanthanide complexes with water. If we assume that each proton in the dimer complex may interact with two metal centers and include a factor of 2 in the relaxation equation, then an equivalently precise fit is obtained with an intermoment distance of 3.1 Å. The correlation time for the rotation of the complex is proportional to the volume of the reorienting unit, which is larger for the dimer than the monomer. However, the correlation time for the high pH complex derived from the inflection point of the dispersion curve is somewhat shorter than those associated with the neutral pH values. This insensitivity of the inflection point to the volume of the complex would be expected if the dimer created a situation where the electron relaxation time became on the order of the rotational correlation time of the dimer. That is, where the electron relaxation time became on the order of 60 ps in the dimer.

One may anticipate that the relaxation in a many-spin system such as this one might become very complex. Indeed, we make no claim that the equations presented here account for all features of the data; however, they do account for the major qualitative features of the data and provide the basis for interpretation that is consistent with the structural chemistry of the complexes and the associated reorientational dynamics. Though caution is required, it is interesting to note that over the pH range up to 9, the data provide no additional hint of more complex behavior. Only one electron relaxation time parameter is needed to account for the shape of the dispersion profile, though it is not clear that only one such relaxation time should be sufficient.[22-26] At pH values over 9, the data are fit less well by a single Lorentzian function. This broadening could arise from a distribution of species or from a complication in the electron relaxation itself.[27,28]

Finally, we note that at pH = 1 the relaxation rate on the high-frequency side of the inflection is approximately 30% that of the low-frequency rate as predicted by Solomon's theory.[20] In all other cases, the data do not agree with the 30% prediction. Nevertheless, the relaxation dispersion profiles are well described by a Lorentzian approximation to the spectral density function, and the parameters that describe the shape and amplitude, namely the correlation time and the intermoment distance, are reasonable. In summary, these data show remarkable consistency over a broad pH range and point to possible advantages of using multimetal paramagnetic centers.

(35) Carrington, A.; McLahlan, A. D. *Introduction to Magnetic Resonance*; Harper and Row: New York, 1967.
(36) Herz, H. G. *Water: A Comprehensive Treatise*; Franks, F., Ed.; Plenum Press: New York, 1973; Chapter 7.
(37) Lippard, S. J.; Schugar, H.; Walling, C. *Inorg. Chem.* **1967**, *6*, 1825.
(38) Banci, L.; Bencini, A.; Dei, A.; Gattesci, D. *Inorg. Chem.* **1981**, *20*, 393.
(39) Bertini, I.; Lanini, G.; Luchinat, C. *J. Magn. Reson.* **1985**, *63*, 56.
(40) Owens, Ch.; Drago, R. S.; Bertini, I.; Luchinat, C.; Banci, L. *J. Am. Chem. Soc.* **1986**, *108*, 3298.
(41) Hudson, A.; Lewis, J. W. E. *Trans. Faraday Soc.* **1970**, *66*, 1297.

Ruthenium Compounds Containing Pyridyltriazines with Low-Lying π* Orbitals

Ronald Hage,[†] John H. van Diemen,[†] Grant Ehrlich,[†] Jaap G. Haasnoot,*,[†] Derk J. Stufkens,[‡] Theo L. Snoeck,[‡] Johannes G. Vos,[§] and Jan Reedijk[†]

A number of ruthenium compounds with 5,6-dimethyl-3-(pyridin-2-yl)-1,2,4-triazine (dmpt), 5,6-diphenyl-3-(pyridin-2-yl)-1,2,4-triazine (dppt), and 3,5,6-tris(pyridin-2-yl)-1,2,4-triazine (tpt) have been prepared. The structures of the complexes have been characterized by using ¹H NMR spectroscopy. The two isolated geometrical isomers of [Ru(dmpt)₃]²⁺ have slightly different electronic properties. The emission, resonance Raman, and electrochemical data show that the LUMO (lowest unoccupied molecular orbital) of all complexes has pyridyltriazine character. A correlation between the electrochemical and absorption/emission data has been observed.

Introduction

Ruthenium compounds with 2,2'-bipyridine (bpy) have been studied extensively because of their potential use as catalysts for the photochemical splitting of water and as redox-catalysts on polymer-modified electrodes.[1-9] Especially ruthenium compounds

† Leiden University.
‡ University of Amsterdam.
§ Dublin City University.

(1) Kalyanasundaram, K.; Gratzel, M.; Pelizetti, E. *Coord. Chem. Rev.* **1986**, *69*, 57.
(2) Seddon, E. A.; Seddon, K. R. *The Chemistry of Ruthenium*; Elsevier: Amsterdam, 1984.
(3) Meyer, T. J. *Pure Appl. Chem.* **1986**, *58*, 1193.
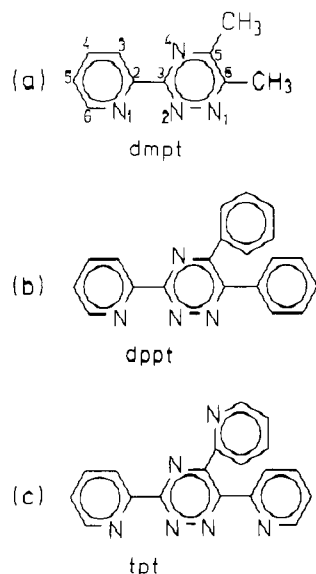
Figure 1. Structure of 5,6-dimethyl-3-(pyridin-2-yl)-1,2,4-triazine = dmpt (a), 5,6-diphenyl-3-(pyridin-2-yl)-1,2,4-triazine = dppt (b), and 3,5,6-tris(pyridin-2-yl)-1,2,4-triazine = tpt (c).

containing symmetrical bipyridine-like ligands, such as substituted bipyridines, phenanthrolines, and biquinolines, have been investigated thoroughly during the last decade.[8,9] Less attention has been paid to ruthenium complexes containing asymmetric bidentate ligands, although compounds have been reported with ligands like pyridylpyrazoles, pyridylbenzimidazoles, pyridyltriazoles, pyridylthiazoles, and pyridylpyrimidine.[10-22] Also, ruthenium compounds containing the ligand 3-(pyridin-2-yl)-5,6-diphenyl-1,2,4-triazine have been prepared.[24] This ligand has been used as a sensitive reagent in the quantitative determination of ruthenium(II) and iron(II).[23-26] However, no systematic study

concerning the synthesis and properties of these complexes has been carried out. In order to obtain more insight into the properties of ruthenium complexes with pyridyltriazines, a series of new ruthenium compounds with various substituted 3-(pyridin-2-yl)-1,2,4-triazines have been prepared (Figure 1). In this study we are in particular interested in establishing whether the pyridyltriazines are directly involved in the emission processes and in the ligand-based reductions or are merely present as spectator ligands.

Experimental Section

Materials. Reagent grade solvents were used as received without further purification. [Ru(bpy)$_2$Cl$_2$]·2H$_2$O was prepared according to literature methods.[27]

Procedure for the Preparation of the Ligands. The ligands 5,6-diphenyl-3-(pyridin-2-yl)-1,2,4-triazine (dppt) and 3,5,6-tris(pyridin-2-yl)-1,2,4-triazine (tpt) were prepared according to literature methods,[28] while 5,6-dimethyl-3-(pyridin-2-yl)-1,2,4-triazine (dmpt) was synthesized in a slightly modified manner (see below).[29] The structure of the ligands is depicted in Figure 1.

5,6-Dimethyl-3-(pyridin-2-yl)-1,2,4-triazine (dmpt) (Figure 1a). Dmpt was prepared by refluxing 0.1 mol of 2-pyridylamidrazone with 0.1 mol of 2,3-butanedione and 0.2 mol of triethylamine in 200 cm^3 of ethanol for 3 h. After evaporation, the dark oil was extracted with hot diisopropyl ether and the extract was left at −20 °C for 2 h. A dark yellow crystalline product was obtained, which was used without further purification. Mp: 197–200 °C. ^{1}H NMR (ppm): 8.76 (d, H6), 8.36 (d, H3), 7.99 (t, H4), 7.55 (t, H5), 2.66 (s, CH$_3$(6)), 2.57 (s, CH$_3$(5)). Yield: 70%.

5,6-Diphenyl-3-(pyridin-2-yl)-1,2,4-triazine (dppt) (Figure 1b). Mp: 185–187 °C (lit. 179–180 °C[28]). ^{1}H NMR (ppm): 8.85 (d, H6), 8.55 (d, H3), 8.07 (t, H4), 7.64 (t, H5), 7.37–7.61 (m, phenyl). Yield: 40%.

3,5,6-Tris(pyridin-2-yl)-1,2,4-triazine (tpt) (Figure 1c). Mp: 183–185 °C (lit. 191–192 °C[28]). ^{1}H NMR (ppm): 8.87 (d, H6), 8.59 (d, H3), 8.08 (t, H4), 7.65 (t, H5), 8.32–8.37 (t, H6′, H6″), 8.10–8.22 (m, H3′, H3″), 7.94–8.05 (m, H4′, H4″), 7.40–7.49 (m, H5′, H5″). Yield: 30%.

Procedure for the Synthesis of the Coordination Compounds. [Ru(bpy)$_2$(tpt)](PF$_6$)$_2$·2H$_2$O (1). A 1-mmol sample of [Ru(bpy)$_2$Cl$_2$] was refluxed with 2.2 mmol of tpt for 6 h in 50 cm^3 of ethanol/water (1/1). After evaporation to dryness, the remaining solid dissolved in 10 cm^3 of water was gradually added to an excess of NH$_4$PF$_6$ solution (3 mmol in 10 cm^3 of water). The precipitate, which was filtered out and dissolved in 5 cm^3 of acetone, was purified by using column chromatography (neutral alumina; ethanol as eluent). The compound was purified by crystallization from water/acetone (1/1) or water/CH$_3$CN (2/1). Yields were in general 60–80%. Anal. Calcd for [Ru(bpy)$_2$(tpt)](PF$_6$)$_2$·2H$_2$O: C, 43.40; H, 3.07; N, 13.32; P, 5.89. Found: C, 43.51; H, 2.10; N, 12.94; P, 5.75.

[Ru(bpy)$_2$(dppt)](PF$_6$)$_2$·H$_2$O·CH$_3$COCH$_3$ (2). This compound was prepared as described for **1**, except now dppt was used. Anal. Calcd for [Ru(bpy)$_2$(dppt)](PF$_6$)$_2$·H$_2$O·CH$_3$COCH$_3$: C, 47.39; H, 3.51; N, 10.28. Found: C, 47.40; H, 3.00; N, 10.52.

[Ru(bpy)$_2$(dmpt)](PF$_6$)$_2$·H$_2$O (3). This compound was prepared as described for **1**, except now dmpt was used. Anal. Calcd for [Ru(bpy)$_2$(dmpt)](PF$_6$)$_2$·H$_2$O: C, 39.70; H, 3.11; N, 12.35; P, 6.83. Found: C, 39.74; H, 2.87; N, 12.15; P, 7.15.

[Ru(dppt)$_3$](PF$_6$)$_2$ (4). A 1-mmol sample of RuCl$_3$·xH$_2$O, 4 mmol of the ligand, and 1 g of L-ascorbic acid were heated in 50 cm^3 of water/ethanol (1/1) for 6 h. After evaporation to dryness, the solid was dissolved in 10 cm^3 of water and the solution was pipetted onto a Sephadex SP-25 column. Elution with 0.3 M NaCl yielded the tris compound. After removal of water, the solid was dissolved again in 10 cm^3 of water and the solution was dropped into an aqueous NH$_4$PF$_6$ solution. The solid was filtered out and washed with water (3 × 10 cm^3 to remove all NaCl). The solid was recrystallized from water/acetone. Anal. Calcd for [Ru(dppt)$_3$](PF$_6$)$_2$: C, 54.51; H, 3.20; N, 12.71; P, 4.69. Found: C, 54.82; H, 3.46; N, 12.65; P, 4.49.

[Ru(dmpt)$_3$](PF$_6$)$_2$ (5). This complex was prepared and purified as described for **4**. After crystallization, different fractions were isolated and characterized (vide infra). Anal. Calcd for [Ru(dmpt)$_3$](PF$_6$)$_2$: C, 37.93; H, 3.16; N, 17.70; P, 6.53. Found: C, 37.82; H, 3.11; N, 17.53; P, 6.72.

Physical Measurements. Electronic absorption spectra were recorded in ethanol on a Perkin-Elmer 330 UV-vis spectrophotometer. Emission spectra were obtained on a Perkin-Elmer LS-5 luminescence spectrophotometer, equipped with a red-sensitive Hamamatsu R928 detector.

(4) Balzani, V.; Boletta, F.; Gandolfi, M. T.; Maestri, M. *Top. Curr. Chem.* **1978**, *75*, 1.

(5) Whitten, D. G. *Acc. Chem. Res.* **1980**, *13*, 83.

(6) Samuels, G. J.; Meyer, T. J. *J. Am. Chem. Soc.* **1981**, *103*, 307.

(7) Haas, O.; Vos, J. G. *J. Electroanal. Chem. Interfacial Electrochem.* **1980**, *113*, 139.

(8) Krause, R. A. *Structure and Bonding*; Springer Verlag: Berlin, 1987; Vol. 67, p 1.

(9) Juris, A.; Balzani, V.; Barigelletti, F.; Belser, P.; von Zelewsky, A. *Coord. Chem. Rev.* **1988**, *84*, 85.

(10) Steel, P. J.; Lahousse, F.; Lerner, D.; Marzin, C. *Inorg. Chem.* **1983**, *22*, 1488.

(11) Marzin, C.; Budde, F.; Steel, P. J.; Lerner, D. *Nouv. J. Chim.* **1987**, *11*, 33.

(12) Haga, M. A. *Inorg. Chim. Acta* **1983**, *75*, 29.

(13) Hage, R.; Haasnoot, J. G.; Reedijk, J.; Vos, J. G. *Inorg. Chim. Acta* **1986**, *118*, 73.

(14) Hage, R.; Prins, R.; Haasnoot, J. G.; Reedijk, J.; Vos, J. G. *J. Chem. Soc., Dalton Trans.* **1987**, 1389.

(15) Hage, R.; Dijkhuis, A. H. J.; Haasnoot, J. G.; Prins, R.; Reedijk, J.; Buchanan, B. E.; Vos, J. G. *Inorg. Chem.* **1988**, *27*, 2185.

(16) Fitzpatrick, L. J.; Goodwin, H. A.; Launikonis, A.; Mau, A. W. H.; Sasse, W. H. F. *Aust. J. Chem.* **1983**, *36*, 2169.

(17) Fitzpatrick, L. J.; Goodwin, H. A. *Inorg. Chim. Acta* **1982**, *61*, 229.

(18) Orellana, G.; Quiroga, M. L.; Braun, A. M. *Helv. Chim. Acta* **1987**, *70*, 2073.

(19) Orellana, G.; Ibarra, C. A.; Santoro, J. *Inorg. Chem.* **1988**, *27*, 1025.

(20) Kitamura, N.; Kawanishi, Y.; Tazuke, S. *Chem. Phys. Lett.* **1983**, *97*, 103.

(21) Haga, M. A. *Inorg. Chim. Acta* **1980**, *45*, L183.

(22) Leidner, C. R.; Sullivan, B. P.; Reed, R. A.; White, B. A.; Crimmins, M. T.; Murray, R. W.; Meyer, T. J. *Inorg. Chem.* **1987**, *26*, 882.

(23) Embry, W. A.; Ayres, G. H. *Anal. Chem.* **1968**, *40*, 499.

(24) Kamra, L. C.; Ayres, G. H. *Anal. Chim. Acta* **1975**, *78*, 423.

(25) Schilt, A. A.; Taylor, P. J. *Anal. Chem.* **1970**, *42*, 220.

(26) Chriswell, C. D.; Schilt, A. A. *Anal. Chem.* **1974**, *46*, 992.

(27) Sullivan, B. P.; Salmon, D. J.; Meyer, T. J. *Inorg. Chem.* **1978**, *17*, 3334.

(28) Case, F. H. *J. Heterocycl. Chem.* **1968**, *5*, 223.

(29) Neuenhoeffer, H.; Weischedel, F. *Liebigs Ann. Chem.* **1971**, *749*, 16.

Table I. ¹H NMR Data for the Pyridyltriazine Ligands of the Ruthenium Compounds

	H3	H4	H5	H6	R
[Ru(bpy)₂(tpt)]²⁺	9.06	8.36	7.84	8.28	7.37 – 8.34[b]
[Ru(bpy)₂(dppt)]²⁺	9.00	8.33	7.80	8.24	7.44 – 8.33[d]
[Bu(bpy)₂(dmpt)]²⁺	8.84	8.27	7.73	8.14	2.71 + 2.47 (CH₃)
[Ru(dppt)₃]²⁺	9.11	8.42	7.85	8.89[d]	7.11 – 7.75[a]
	8.84	8.37	7.83	8.47[d]	
	8.96	8.42	7.98	8.85[d]	
	8.98	8.42	7.75	8.60[e]	
[Ru(dmpt)₃]²⁺	8.85	8.33	7.76	8.46[d]	2.49 + 2.74[e]
	8.74	8.25	7.64	8.20[d]	
	8.66	8.25	7.71	8.09[d]	
	8.82	8.35	7.81	8.52[e]	2.45 + 2.76[e]
[Ru(bpy)₃]²⁺	8.90	8.12	7.53	7.71	

[a] R = phenyl. [b] R = pyridine. [c] R = CH₃. [d] From *mer* isomer. [e] From *fac* isomer.

Emission intensities were not corrected for photomultiplier response. The ¹H NMR spectra were obtained on a JEOL JNM-FX 200 NMR spectrometer. The measurements of the ligands were carried out in DMSO-d_6, while the NMR spectra of the metal complexes were obtained in acetone-d_6. The peak positions are relative to TMS. For the COSY experiments, 256 FID's of eight scans each, consisting of 1K data points, were accumulated. After digital filtering (sine bell squared), the FID was zero-filled to 512 W in the F_1 dimension. Acquisition parameters were F_1 = ±500 Hz, F2 = 1000 Hz, and $t_{1/2}$ = 0.001 s; the cycle decay was 1.5 s.

The cyclic voltammograms and differential pulse polarographic measurements were carried out on an EG&G PAR C Model 303 with an EG&G 384B polarographic analyzer. The scan rate was 4 mV/s with a pulse height of 20 mV. A saturated calomel electrode (SCE) was used as reference electrode; all measurements were performed by using a platinum electrode. The solvent used was CH₃CN (spectroscopic grade) with 0.1 M tetrabutylammonium perchlorate (TBAP) as supporting electrolyte. Before all measurements, the solution was purged thoroughly with argon gas. Elemental analyses were carried out at University College, Dublin. The resonance Raman spectra were recorded in CH₃-CN solution by using a spinning cell and a Jobin Yvon HG2S Ramanor spectrophotometer. The samples were excited by the 458-, 476.5-, 488-, and 514.5-nm lines of an SP Model 171 argon ion laser. Laser power was 50–100 mW, and spectral slit width, ca. 10 cm⁻¹.

Results and Discussion

Nuclear Magnetic Resonance Spectroscopy. Because it has previously been shown that NMR spectroscopy can play an important role in determing the purity and coordination geometry of ruthenium complexes, all reported compounds were analyzed by using high-resolution ¹H NMR spectroscopy.[10,11,13-15,30-35] The complexity of the spectra made it necessary to carry out COSY experiments to assign the spectra.[15] ¹H NMR data for the ruthenium compounds are listed in Table I. Chemical shifts of the bpy ligands in the mixed-ligand complexes have been omitted because of their similarity to those reported previously for similar compounds.[14] The assignment of the shifts of the protons of the pyridyltriazine ligands in the mixed-ligands complexes was performed by comparison with the chemical shifts of the protons in [Ru(bpy)₃]²⁺ (Table I).

As reported previously, octahedral complexes with three bidentately coordinating ligands can exist as facial (*fac*) or as meridional (*mer*) isomers.[13] For [Ru(dmpt)₃]²⁺, two fractions were isolated: one containing very pure (>95%) *mer* isomer and the second fraction containing pure *fac* isomer. The properties of these isomers will be discussed in the next sections. In the *fac* isomer, the three ligands are magnetically equivalent (C_3 axis),

(30) Belser P.; von Zelewsky, A. *Helv. Chim. Acta* **1980**, *63*, 1675.
(31) Bryant, G. M.; Fergusson, J. E. *Aust. J. Chem.* **1971**, *24*, 441.
(32) Lytle, F. E.; Petrosky, M.; Carlson, L. R. *Anal. Chim. Acta* **1971**, *57*, 239.
(33) Cook, M. J.; Lewis, A. P.; McAuliffe, G. S. G.; Thomson, A. J. *Inorg. Chim. Acta* **1982**, *64*, L25.
(34) Walsh, L. J.; Durham, B. *Inorg. Chem.* **1982**, *21*, 329.
(35) Clear, J. M.; Kelly, J. M.; O'Connell, C. M.; Vos, J. G. *J. Chem. Res., Miniprint* **1981**, 3039.
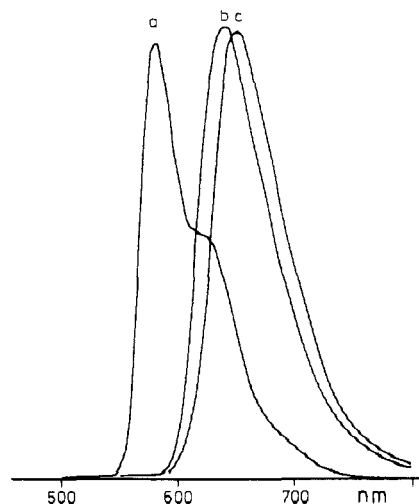
Figure 2. Emission spectra of [Ru(bpy)₃]²⁺ (a), [Ru(dppt)₃]²⁺ (b), and [Ru(bpy)₂(dppt)]²⁺ (c) measured at 80 K in methanol.

yielding only one set of protons in the NMR spectrum. However, in the *mer* isomer, the three bidentate ligands are not equivalent, which results in the presence of three different sets of protons in the NMR spectrum (Table I). Since for [Ru(dppt)₃](PF₆)₂ only a mixture of *fac* and *mer* isomers was isolated, the proton NMR spectrum proved to be very complicated, as it contains signals for four sets of protons for the pyridyltriazine ligands. The assignment for the *fac* and *mer* isomers was carried out by comparing the intensities of the four sets of peaks, the three peaks of the *mer* isomer having the same intensity. The coordination mode of the pyridyltriazine ligands is as expected via N2 of the triazine ring and via the pyridine nitrogen atom. In this case much less steric hindrance between the R groups and adjacent ligands is present. The chemical shifts of the protons of the R groups (CH₃, phenyl, or pyridiyl) are not changed much upon coordination, indicating that steric hindrance is not present to a large extent.

Absorption and Emission Data. The positions of the lowest energy metal-to-ligand charge-transfer (MLCT) bands, the emission maxima, and the oxidation and reduction potentials of the various compounds are listed in Table II. On the basis of the absorption spectra, the ruthenium complexes with the pyridyltriazine ligands can be divided into two classes: (a) in the dppt and tpt complexes (entries 1, 2, and 4 in Table II) the MLCT bands are shifted to lower energy compared to those of the well-studied [Ru(bpy)₃]²⁺ cation (see also Figure 2, and (b) in the dmpt complexes (entries 3, 5a, and 5b in Table II) the MLCT bands are observed at higher energy than those for [Ru(bpy)₃]²⁺. All ruthenium compounds show emission both at 77 K and at room temperature. The emission signals obtained for [Ru(bpy)₂(tpt)]²⁺ at liquid nitrogen temperature and at room temperature and for [Ru(bpy)₂(dppt)]²⁺ at room temperature are very weak. Therefore, the emission maxima obtained for these complexes are less accurate.

A number of distinct differences between [Ru(bpy)₃]²⁺ and the compounds reported here are observed. The emission maxima of the pyridyltriazine compounds are found at lower energy than those of [Ru(bpy)₃]²⁺. Figure 2 shows that the low-temperature emission of [Ru(bpy)₂(dppt)]²⁺ is quite different from that of [Ru(bpy)₃]²⁺, but closely resemblances that of [Ru(dppt)₃]²⁺. This suggests that the emission in [Ru(bpy)₂(dppt)]²⁺ occurs from the ³MLCT levels of the phenyl-substituted pyridyltriazine ligand rather than from bipyridyl-based orbitals.

More detailed analyses are necessary to fully reveal the emission properties of these systems.

Electrochemical Data. For the ruthenium complexes containing dipyridyl- or diphenyl-substituted pyridyltriazine as ligands, the Ru^II/III oxidation potentials have been shifted to more positive values compared to those of [Ru(bpy)₃]²⁺, while the ligand-based reduction potentials are observed at less negative values (Table II). This has been observed for the [Ru(LL′)₃]²⁺ compounds as well as the [Ru(bpy)₂(LL′)]²⁺ complexes. The first reduction

Table II. Absorption, Emission, and Electrochemical Data for the Ruthenium Compounds[a]

entry	compd[b]	abs data, λ_{max}, nm (ϵ, 10^4 M^{-1} cm^{-1})		emission data, nm room temp	77 K	electrochemical data, V oxidn pot.	redn pot.			$\Delta E_{1/2}$
1	[Ru(bpy)₂(tpt)]²⁺	484 (1.44)	420 (sh)	670	680	+1.41	−0.80	−1.44	−1.73	2.21
2	[Ru(bpy)₂(dppt)]²⁺	477 (1.92)	430 (sh)	690	655	+1.34	−0.85	−1.35		2.19
3	[Ru(bpy)₂(dmpt)]²⁺	442 (1.41)	434 (sh)	656	620	+1.30	−1.18	−1.52	−1.77	2.48
4	[Ru(dppt)₃]²⁺	470 (3.44)		650	642	+1.49	−0.90	−1.04	−1.37	2.39
5a	*mer*-[Ru(dmpt)₃]²⁺	442 (2.08)		625	595	+1.43	−1.15	−1.36	−1.64	2.58
5b	*fac*-[Ru(dmpt)₃]²⁺	434 (2.01)		620	595	+1.47	−1.14	−1.33	−1.59	2.61
6	[Ru(bpy)₃]²⁺	452 (1.29)		608	582	+1.22	−1.36	−1.53		2.58

[a] Measured in ethanol. [b] Numbers refer to points in Figure 3.

potential of [Ru(bpy)₂(dppt)]²⁺ is approximately the same as that of [Ru(dppt)₃]²⁺, while the second reduction potential of [Ru-(bpy)₂(dppt)]²⁺ is the same as the first reduction potential of [Ru(bpy)₃]²⁺.

Compared with the analogous dppt and tpt compounds, the oxidation potentials of [Ru(dmpt)₃]²⁺ and [Ru(bpy)₂(dmpt)]²⁺ are similar, but the first reduction wave is observed at a much more negative potential. This indicates that the difference between the lowest π* level and filled d orbitals is larger in the case of the complexes with dmpt.[36-46] However, the reduction potentials of [Ru(dmpt)₃]²⁺ and [Ru(bpy)₂(dmpt)]²⁺ are still less negative than the first reduction potential of [Ru(bpy)₃]²⁺, which effect is also evident from the resonance Raman data, as will be discussed hereafter.

[Ru(dmpt)₃]²⁺ has been isolated as pure *fac* and pure *mer* isomers (see Nuclear Magnetic Resonance section). Interestingly, the absorption maximum of the MLCT band of *fac*-[Ru(dmpt)₃]²⁺ is different from that of the *mer* isomer (see Table II). Also some differences in electrochemical potentials have been observed. This is unlike the observation made with the *fac* and *mer* ruthenium complexes with 1-methyl-3-(pyridin-2-yl)-1,2,4-triazole. For this compound, the absorption maxima and electrochemical data are essentially the same.[13] No pure *fac*- and *mer*-[Ru(dppt)₃]²⁺ have been isolated, and therefore, the properties of the *fac* and *mer* isomers of this compound could not be evaluated.

Correlation between Electronic and Electrochemical Data. In Figure 3, the absorption and emission maxima (in eV) versus the difference between oxidation and reduction potential are depicted. Apart from data for the ruthenium compounds with pyridyltriazines, some data are also listed for ruthenium complexes with pyridyltriazoles reported previously.[14] The absorption and emission maxima of the ruthenium compounds with dppt and tpt correlate well with the electrochemical measurements. A similar correlation has been reported previously for other ruthenium systems, and this can be explained by assuming that the same type of orbitals play a role in the absorption and emission processes as well as the oxidation and reduction processes of the complexes.[9,14,43-45] In a MLCT absorption process, an electron is removed from the filled metal orbital (dπ) to an empty orbital of the ligand (π*). Oxidation is also removal of an electron from the d orbitals, and by reduction, an electron is transferred to the LUMO (lowest
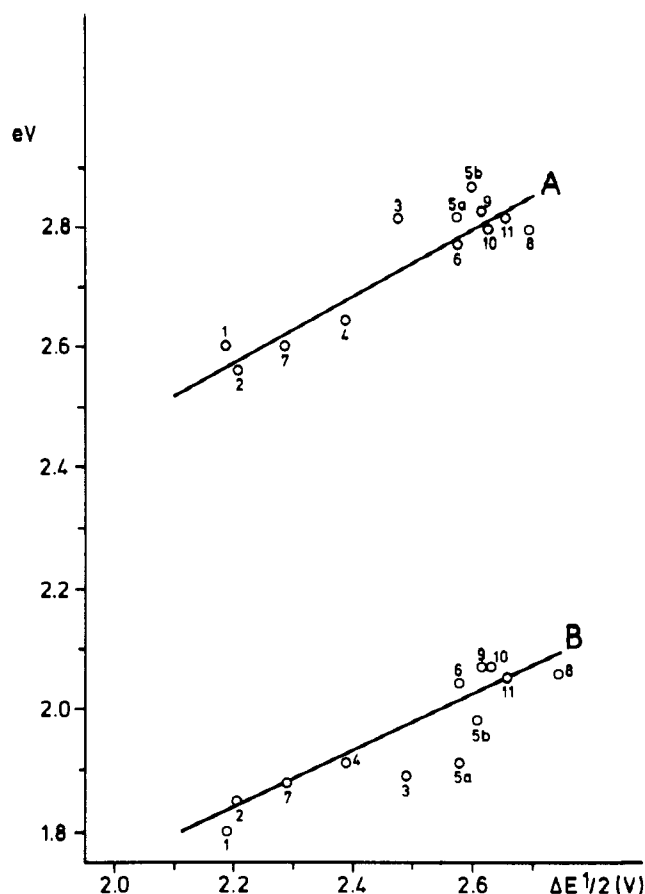
Figure 3. Correlation between $\Delta E_{1/2}$ ($=E_{ox} - E_{red}$) and the energy of the absorption (A) and emission (B) maxima as measured in ethanol at room temperature. Points 1–6 refer to the compounds presented in Table II, while points 7–11 are for [Ru(bpy)₂(5Mptr)]⁺, [Ru(bpy)₂(5MHptr)]²⁺, [Ru(bpy)₂(4Mptr)]²⁺, [Ru(bpy)₂(1Mptr)]²⁺, and [Ru(bpz)₃]²⁺ taken from refs 14 and 9.

unoccupied molecular orbital) of the complex. A similar explanation is also valid for the MLCT emission processes.[37]

The electrochemical and emission measurements indicate that the lowest π* level of the various complexes are pyridyltriazine-based. The LUMO and HOMO (highest occupied molecular orbital) of the ruthenium complexes with the pyridyltriazine are stabilized compared to those of [Ru(bpy)₃]²⁺. Similar shifts have been observed previously for ruthenium(II) compounds containing 3,3'-bipyridazine, 4,4'-bipyrimidine, 2,2'-bipyrazine, and 2,2'-bipyrimidine.[38-42] It has been argued that, for those complexes, the π* levels are lowered (stronger π-acceptor properties), while the σ-donor properties are weaker compared to those of the analogous bpy complexes. Therefore, the ruthenium(III) species are less stabilized, and the oxidation potentials are shifted to higher values. Hückel calculations indicated that this explanation is valid; the LUMO of the pyridyltriazine ligand with pyridine or phenyl as substituent is lower than those of 2,2'-pyridine, 3,3'-bipyridine, 4,4'-bipyrimidine, 2,2'-bipyrazine, and 2,2'-bipyrimidine. However,

(36) Juris, A.; Barigelletti, F.; Balzani, V.; Belser, P.; von Zelewsky, A. *Inorg. Chem.* **1985**, *24*, 204.
(37) Ernst, S.; Kaim, W. *Inorg. Chem.* **1989**, *28*, 1520.
(38) (a) Kaim, W. *J. Am. Chem. Soc.* **1982**, *104*, 3833. (b) Ernst, S. Ph.D. Dissertation, Frankfurt am Main, 1987.
(39) Rillema, D. P.; Allen, G.; Meyer, T. J.; Conrad, D. *Inorg. Chem.* **1983**, *22*, 1617.
(40) Rillema, D. P.; Mack, K. B. *Inorg. Chem.* **1982**, *21*, 3849.
(41) Rillema, D. P.; Callahan, R. W.; Mack, K. B. *Inorg. Chem.* **1982**, *21*, 2589.
(42) Crutchley, R. J.; Lever, A. B. P. *Inorg. Chem.* **1982**, *21*, 2276.
(43) Williams, R. J. P. *J. Chem. Soc.* **1955**, 137.
(44) Casper, J. V.; Meyer, T. J. *Inorg. Chem.* **1983**, *22*, 2444.
(45) (a) Barigelletti, F.; Juris, A.; Balzani, V.; Belser, P.; von Zelewsky, A. *Inorg. Chem.* **1987**, *26*, 4115. (b) Dodsworth, E. S.; Lever, A. B. P. *Chem. Phys. Lett.* **1986**, *124*, 152.
(46) A local PC program for Hückel calculations on aromatic π systems was used, written by E. Müller, Leiden University, 1989.
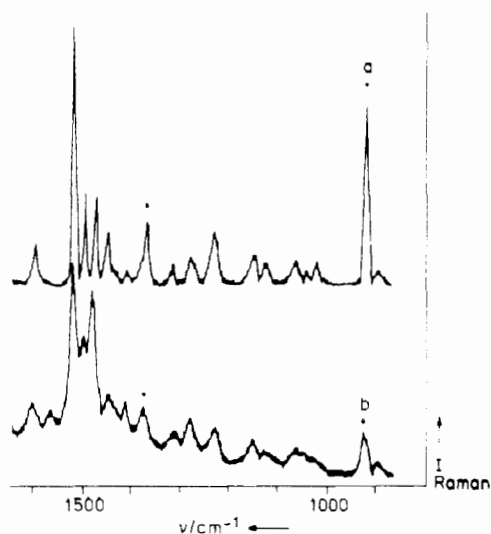
Figure 4. Resonance Raman spectra of $[Ru(dppt)_3]^{2+}$. λ_{exc}: 514.5 nm (a); 458 nm (b). Bands marked with a • are solvent bands.

for the methyl-substituted pyridyltriazine ligand, the LUMO is somewhat higher in energy than that of the phenyl- or pyridine-substituted pyridyltriazine ligand, and its value is comparable to the LUMO of bipyrazine.[46]

Resonance Raman Measurements. From the various experiments (electrochemistry, Hückel calculations, and absorption and emission spectroscopy), it was concluded that the LUMO of the mixed-ligand complexes is localized at the pyridyltriazine ligand. In order to confirm this conclusion, resonance Raman (rR) spectra of all complexes have been recorded. Such spectra are often used to assign electronic transitions.[47-51] If excitation takes place into an allowed electronic transition, the rR spectra are characterized by strong rR effects for the vibrations of those bonds that are mostly affected by the electronic transition. Thus, excitation into an allowed Ru → π* (α-diimine) transition primarily affects the ligand bonds, and as a result, enhancement of Raman intensity is normally observed for the symmetrical stretching modes of the α-diimine ligand. With this method, different electronic transitions within one absorption band can also be detected and identified by studying the wavelength dependence of the rR spectra.[51] It will be shown hereafter how these rR spectra can be used to assign the low-energy absorption bands of the mixed-ligand complexes $[Ru(bpy)_2(LL')]^{2+}$ in relationship to those of $[Ru(bpy)_3]^{2+}$ and $[Ru(LL')_3]^{2+}$.

Excitation with the 514.5-nm laser line at the low-energy side of the MLCT band of $[Ru(dppt)_3]^{2+}$ (λ_{max} = 470 nm) gave rise to rR effects for ligand stretching modes at 1606, 1570, 1554, 1523, 1486, and 1267 cm^{-1}, which are in the same region as the bpy vibrations.[47] When excitation takes place at the high-energy side of this band (λ_{exc} = 458 nm), the relative intensities of some of the Raman bands change (see Figure 4), most probably because of the presence of a second MLCT transition within the absorption band originating from different metal d orbitals.

Excitation of $[Ru(bpy)_2(dppt)]^{2+}$ with the 514.5- and 488-nm laser lines at the low-energy side of the absorption band gave rise to resonance enhancement of dppt stretching modes only, while two additional bands at 1560 and 1480 cm^{-1} belonging to bpy vibrations[47] showed up in the 458-nm-excited spectrum (Figure 5). Apparently, the 477-nm band of this complex belongs to one or more Ru → dppt transitions, and shoulder at 430 nm, to a

(47) Mabrouk, P. A.; Wrighton, M. S. *Inorg. Chem.* **1986**, *25*, 526.
(48) Basu, A.; Gafney, H. D.; Strekas, T. C. *Inorg. Chem.* **1982**, *21*, 2231.
(49) Braunstein, C. H.; Baker, A. D.; Strekas, T. C.; Gafney, H. D. *Inorg. Chem.* **1984**, *23*, 857.
(50) Tait, C. D.; Donohoe, R. J.; DeArmond, M. K.; Wertz, D. W. *Inorg. Chem.* **1987**, *26*, 2754.
(51) (a) Stufkens, D. J.; Snoeck, T. L.; Lever, A. B. P. *Inorg. Chem.* **1988**, *27*, 953. (b) Servaas, P. C.; van Dijk, H. K.; Snoeck, T. L.; Stufkens, D. J.; Oskam, A. *Inorg. Chem.* **1985**, *24*, 4494.
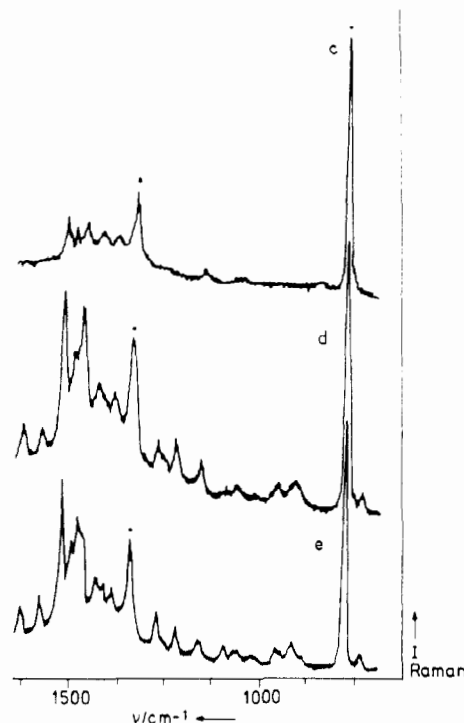
Figure 5. Resonance Raman spectra of $[Ru(bpy)_2(dppt)]^{2+}$. λ_{exc}: 514.5 nm (c); 488 nm (d); 458 nm (e). Bands marked with a • are solvent bands.

transition or transitions from Ru to bpy.

A similar wavelength dependence was observed for the rR spectra of $[Ru(bpy)_2(tpt)]^{2+}$. Only upon excitation with the 458-nm line at the high-energy side of the MLCT band (λ_{max} = 484 nm) were bpy vibrations observed (1609, 1565, and 1483 cm^{-1}, respectively). Also in this case, the main absorption band belongs to one or more Ru → tpt transitions, while the shoulder at 420 nm belongs to transitions directed to bpy. Unfortunately, these spectra could not be compared with those of $[Ru(tpt)_3]^{2+}$, since this complex could not be isolated as a pure compound (vide supra).

The rR spectra of *fac*- and *mer*-$[Ru(dmpt)_3]^{2+}$ were very similar. This agrees with the observation that the reduction potentials are nearly the same (Table II), and that the same π* orbitals are involved in the absorption and emission processes.

The rR spectrum of $[Ru(bpy)_2(dmpt)]^{2+}$, obtained by excitation with the 514.5-nm line was very similar to that of $[Ru(dmpt)_3]^{2+}$. Again, bpy vibrations (1563 and 1483 cm^{-1}) were only observed upon excitation at higher energy (λ_{max} = 458 nm).

These results clearly show that, for all three mixed-ligand complexes under study, the transitions to LL' are at the low-energy side and those to bpy at the high-energy side of the MLCT band. The resonance Raman measurements also indicate that, in the three mixed-ligand complexes, the first reduction potential is pyridyltriazine-based, which is in agreement with the electrochemical measurements.

Concluding Remarks. A series of new ruthenium complexes with three differently substituted pyridyltriazines have been prepared and characterized. The structure of the complexes has been determined by using NMR spectroscopy. The resonance Raman measurements and electrochemical data suggest that the pyridyltriazine ligands have rather low-lying LUMO levels. Furthermore, the σ-donor properties of the ligands are weaker than those of bpy, causing higher oxidation potentials. Both the $[Ru(LL')_3]^{2+}$ and the $[Ru(bpy)_2(LL')]^{2+}$ compounds show emission maxima both at room temperature and at 77 K. A correlation with the difference between the oxidation and reduction potentials of the complexes and the absorption and emission maxima is observed. These results suggest that the properties of these new compounds can be well understood by a simple orbital diagram, as reported previously for other ruthenium compounds.[9] From these results it can be concluded that the pyridyltriazine

ligands are not merely spectator ligands, but participate actively in the photophysical processes.

Contribution from the Department of Chemistry, The University of Mississippi, University, Mississippi 38677

Electrochemistry and Spectroelectrochemistry of Polynuclear Rhenium(III) Chloride Cluster Complexes and Their One-Electron-Reduction Products in a Basic Room-Temperature Chloroaluminate Molten Salt

Sandra K. D. Strubinger, I-Wen Sun, Walter E. Cleland, Jr., and Charles L. Hussey*

The dimeric, metal–metal-bonded rhenium(III) complex $[Re_2Cl_8]^{2-}$ is stable in the basic aluminum chloride–1-methyl-3-ethylimidazolium chloride ($AlCl_3$–MeEtimCl) molten salt and can be reduced to $[Re_2Cl_8]^{3-}$ at a glassy-carbon electrode in a reversible electrode reaction with a voltammetric half-wave potential, $E_{1/2}$, of ca. –0.58 V in the 49.0/51.0 mol % melt versus the Al^{3+}/Al couple in the 66.7/33.3 mol % melt at 40 °C. It is possible to electrochemically generate stable, bulk solutions containing $[Re_2Cl_8]^{3-}$, provided that oxygen is rigorously excluded from the electrochemical cell. The average Stokes–Einstein products for $[Re_2Cl_8]^{2-}$ and $[Re_2Cl_8]^{3-}$ are 2.0×10^{-10} and 1.2×10^{-10} g cm s^{-2} K^{-1}, respectively. The addition of Re_3Cl_9 to basic $AlCl_3$–MeEtimCl produces the trimeric, metal–metal-bonded rhenium(III) complex $[Re_3Cl_{12}]^{3-}$. This species can also be reduced at a glassy-carbon electrode in a one-electron, reversible electrode reaction with an $E_{1/2}$ of about –0.34 V in this same basic melt. However, $E_{1/2}$ for this reaction is dependent upon the pCl of the melt, indicating the loss of chloride ion from the coordination sphere of the cluster during reduction to form a species of the type $[Re_3Cl_{12-x}]^{(4-x)-}$ for which x may be 1. It is possible to electrochemically generate stable solutions of this reduced species in the absence of oxygen. The average Stokes–Einstein products for $[Re_3Cl_{12}]^{3-}$ and its one-electron-reduction product are 1.3×10^{-10} and 1.0×10^{-10} g cm s^{-2} K^{-1}, respectively. Both $[Re_2Cl_8]^{2-}$ and $[Re_3Cl_{12}]^{3-}$ exhibit an additional multielectron voltammetric reduction process at potentials negative of their one-electron reduction waves. In both cases, bulk electrolysis experiments conducted at potentials negative of these very large waves destroyed the parent clusters. In basic melt at temperatures of ca. 175 °C or more, each $[Re_3Cl_{12}]^{3-}$ ion is irreversibly converted to one $[Re_2Cl_8]^{2-}$ ion. Absorption spectroscopic data for $[Re_2Cl_8]^{2-}$, $[Re_3Cl_{12}]^{3-}$, and their one-electron-reduction products are reported.

Introduction

The combination of aluminum chloride and certain quaternary ammonium chloride salts, notably 1-(1-butyl)pyridinium chloride (BupyCl) or 1-methyl-3-ethylimidazolium chloride (MeEtimCl), produces molten salts or ionic liquids that are molten at room temperature.[1] The Lewis acid–base properties of these chloroaluminate molten salts can be controlled by adjusting the ratio of aluminum chloride to organic salt. Those melts containing a molar excess of aluminum chloride are designated as "acidic" because they have been shown to contain the chloride ion acceptor $Al_2Cl_7^-$ while those containing a molar excess of the organic chloride salt are considered to be basic because they contain chloride ion that is not covalently bound to aluminum. Basic room-temperature chloroaluminate ionic liquids have been shown to be expedient solvents for studying the electrochemistry and absorption spectroscopy of a wide variety of highly charged anionic transition-metal chloride complexes;[2] in many cases they have proven to be superior to conventional molecular solvents like water, acetonitrile, and dichloromethane and to high-temperature molten salts like the alkali-metal chlorides and the alkali-metal chloride based chloroaluminates. The important factors that contribute to the utility of these molten salts as solvents for characterizing these complexes have been discussed at length.[2,3] One disadvantage of room-temperature chloroaluminate molten salts is that they and their components are extremely moisture sensitive and must be handled only in a glovebox with a very dry atmosphere or in sealed vessels.

Metal–metal-bonded, polynuclear transition-metal clusters, which are differentiated from classical polynuclear species or Werner complexes in which the component metal atoms may share ligands but do not otherwise interact, are of great interest as a result of their bonding, structures, and reactivities. The chemistry of rhenium(III) is especially fertile with regard to polynuclear metal clusters, and two anionic chloride cluster complexes, $[Re_2Cl_8]^{2-}$ and $[Re_3Cl_{12}]^{3-}$, are well-known. The former complex possesses a quadruple metal–metal bond with a Re–Re distance of about 0.22 nm[4] while the latter, which exists as a triangular arrangement of metal atoms with two sets of double bonds per atom, exhibits a slightly longer Re–Re separation of about 0.25 nm.[5]

Reports describing the electrochemistry of $[Re_2Cl_8]^{2-}$ are conflicting. For example, Cotton and co-workers[6] reported two one-electron polarographic reduction waves for $[Re_2Cl_8]^{2-}$ in acetonitrile at a dropping-mercury electrode (DME). A later cyclic voltammetric study of this complex by Hendriksma and van Leeuwen[7] at a hanging-mercury-drop electrode (HMDE) also revealed two one-electron reduction processes. The first reduction reaction was reported to be electrochemically reversible, but the product of this reaction was only moderately stable on the voltammetric time scale while the two-electron-reduction product was found to be completely unstable. A subsequent voltammetric examination of $[Re_2Cl_8]^{2-}$ at a platinum electrode in both acetonitrile and dichloromethane revealed only a *single* one-electron, quasireversible electrode reaction.[8] The one-electron-reduction

(1) For reviews see: (a) Chum, H. L.; Osteryoung, R. A. In *Ionic Liquids*; Inman, D., Lovering, D. G., Eds.; Plenum: New York, 1981; pp 407–423. (b) Hussey, C. L. *Adv. Molten Salt Chem.* **1983**, *5*, 185–230. (c) Gale, R. J.; Osteryoung, R. A. In *Molten Salt Techniques*; Lovering, D. G., Gale, R. J., Eds.; Plenum: New York, 1983; Vol. 1, pp 55–78.
(2) Hussey, C. L. *Pure Appl. Chem.* **1988**, *60*, 1763.
(3) Appleby, D.; Hussey, C. L.; Seddon, K. R.; Turp, J. E. *Nature* **1986**, *323*, 614.

(4) Cotton, F. A.; Walton, R. A. *Multiple Bonds Between Metal Atoms*; Wiley: New York, 1982; pp 40–41.
(5) See ref 4, pp 266–267.
(6) Cotton, F. A.; Robinson, W. R.; Walton, R. A. *Inorg. Chem.* **1967**, *6*, 1257.
(7) Hendriksma, R. R.; van Leeuwen, H. P. *Electrochim. Acta* **1973**, *18*, 39.
(8) Cotton, F. A.; Pedersen, E. *Inorg. Chem.* **1975**, *14*, 383.